LETTER

doi:10.1038/nature11986

Succinate is an inflammatory signal that induces IL-1β through HIF-1α

G. M. Tannahill[1], A. M. Curtis[1], J. Adamik[2], E. M. Palsson-McDermott[1], A. F. McGettrick[1], G. Goel[3], C. Frezza[4,5], N. J. Bernard[1], B. Kelly[1], N. H. Foley[1], L. Zheng[4], A. Gardet[6], Z. Tong[7], S. S. Jany[1], S. C. Corr[1], M. Haneklaus[1], B. E. Caffrey[8], K. Pierce[6], S. Walmsley[9], F. C. Beasley[10], E. Cummins[11], V. Nizet[10], M. Whyte[9], C. T. Taylor[11], H. Lin[7], S. L. Masters[12], E. Gottlieb[4], V. P. Kelly[1], C. Clish[6], P. E. Auron[2]*, R. J. Xavier[3,5]* & L. A. J. O'Neill[1]

Macrophages activated by the Gram-negative bacterial product lipopolysaccharide switch their core metabolism from oxidative phosphorylation to glycolysis[1]. Here we show that inhibition of glycolysis with 2-deoxyglucose suppresses lipopolysaccharide-induced interleukin-1β but not tumour-necrosis factor-α in mouse macrophages. A comprehensive metabolic map of lipopolysaccharide-activated macrophages shows upregulation of glycolytic and down-regulation of mitochondrial genes, which correlates directly with the expression profiles of altered metabolites. Lipopolysaccharide strongly increases the levels of the tricarboxylic-acid cycle intermediate succinate. Glutamine-dependent anerplerosis is the principal source of succinate, although the 'GABA (γ-aminobutyric acid) shunt' pathway also has a role. Lipopolysaccharide-induced succinate stabilizes hypoxia-inducible factor-1α, an effect that is inhibited by 2-deoxyglucose, with interleukin-1β as an important target. Lipopolysaccharide also increases succinylation of several proteins. We therefore identify succinate as a metabolite in innate immune signalling, which enhances interleukin-1β production during inflammation.

Activation of Toll-like receptors, notably Toll-like receptor 4, leads to a switch from oxidative phosphorylation to glycolysis in immune cells[1,2], similar to that occurring in tumours. In bone-marrow-derived macrophages (BMDMs), 2-deoxyglucose (2DG) specifically inhibits lipopolysaccharide (LPS)- and *Bordetella pertussis*-induced interleukin-1β (*Il1b*) transcription, but not tumour-necrosis factor-α (*Tnf*) (Fig. 1a, b) or interleukin-6 (*Il6*) (Supplementary Figs 1 and 2) transcription. 2DG had no effect on invasion and growth of the bacteria in BMDMs (Supplementary Fig. 3). The inhibitory effect of 2DG on LPS-induced IL-1β was evident *in vivo*. Inhibition of TNF-α *in vivo* was also evident, most probably because of an IL-1β-dependency on induction of TNF-α (Fig. 1c). There was no effect on the induction of IL-6 *in vivo* (Supplementary Fig. 4).

Supplementary Fig. 5 lists LPS-regulated genes affected by 2DG, including *Il1b*. Several hypoxia-inducible factor-1α (HIF-1α) targets were upregulated by LPS and downregulated with 2DG, including ankyrin repeat domain 37, lysyl oxidase and activating transcription factor 3.

LPS-induced HIF-1α protein but not messenger RNA expression in BMDMs was inhibited by 2DG (Fig. 2a and Supplementary Fig. 6). To examine a direct functional relationship between HIF-1α and IL-1β, we found LPS-induced IL-1β protein expression was markedly increased under hypoxia (Fig. 2b), TNF-α was not affected and, as previously shown[3], IL-6 expression was inhibited (Supplementary Fig. 7). The prolyl hydroxylase (PHD) inhibitor dimethyloxallyl glycine, which stabilizes HIF-1α protein, also boosted LPS-induced *Il1b* mRNA (Supplementary Fig. 8). Conversely, pre-treating LPS-stimulated BMDMs with a cell-permeable α-ketoglutarate (α-KG) derivative, which increases PHD activity, depleting HIF-1α, significantly reduced LPS-induced *Il1b* mRNA (Fig. 2c). α-KG inhibited expression of both LPS-induced HIF-1α and IL-1β protein in a dose-dependent manner

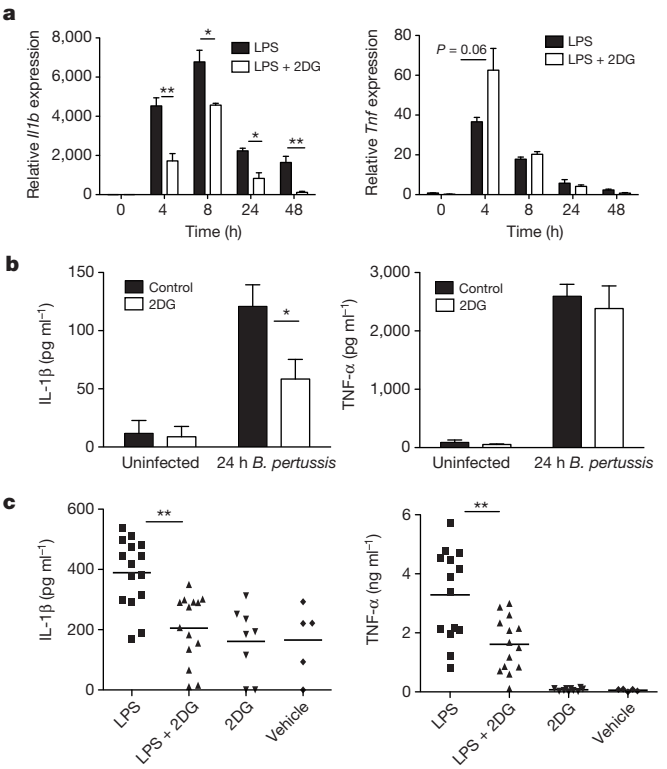

Figure 1 | Glycolysis is necessary for LPS-induced IL-1β expression. **a**, **b**, *Il1b* and *Tnf* messenger RNA in 100 ng ml^{-1} LPS- or 1×10^5 *B. pertussis*-stimulated BMDMs ± 2DG (1 mM) pre-treatment for 3 h ($n = 3$). **c**, Mice injected intraperitoneally with or without 2DG (2 g kg^{-1}) or PBS for 3 h, then 15 mg kg^{-1} LPS or PBS for 1.5 h. Serum concentrations of IL-1β and TNF-α: LPS, $n = 15$; LPS + 2DG, $n = 14$; 2DG, $n = 8$; vehicle, $n = 5$. Error bars, s.e.m. $^*P < 0.05$; $^{**}P < 0.01$.

[1]School of Biochemistry and Immunology, Trinity Biomedical Sciences Institute, Trinity College Dublin, Dublin 2, Ireland. [2]Department of Biological Sciences, Duquesne University, Pittsburgh, Pennsylvania 15282, USA. [3]Centre for Computational and Integrative Biology, Massachusetts General Hospital, Richard B. Simches Research Center, Boston, Massachusetts 02114, USA. [4]Apoptosis and Tumour Physiology Laboratory, The Beatson Institute for Cancer Research, Bearsden, Glasgow G61 1BD, UK. [5]Medical Research Council Cancer Cell Unit Hutchison/MRC Research Centre, Hills Road, Cambridge CB2 0X2, UK. [6]The Broad Institute of MIT and Harvard, 7 Cambridge Center, Cambridge, Massachusetts 02142, USA. [7]Department of Chemistry and Chemical Biology, Cornell University, Ithaca, New York 14853, USA. [8]Smurfit Institute of Genetics, Trinity College Dublin, Dublin 2, Ireland. [9]Academic Unit of Respiratory Medicine, Department of Infection and Immunity, University of Sheffield, Sheffield S10 2RX, UK. [10]V. Nizet Laboratory, Division of Pediatrics, Centre for Neural Circuits and Behaviour, University of California, La Jolla, California 92093-0687, USA. [11]Conway Institute, University College Dublin, Dublin 4, Ireland. [12]Inflammation Division, Walter and Eliza Hall Institute, 1G Royal Parade, Parkville, Victoria 3052, Australia.
*These authors contributed equally to this work.

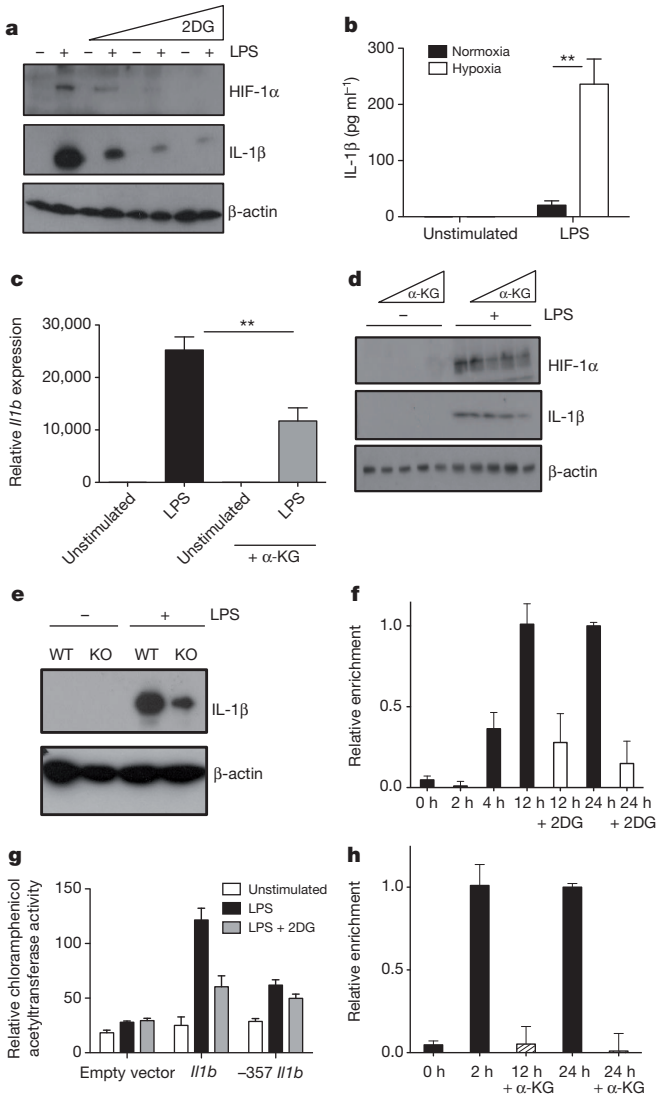

Figure 2 | HIF-1α is responsible for LPS-induced IL-1β expression. **a**, LPS-induced HIF-1α and IL-1β protein expression with or without 2DG (1, 5, 10 mM). **b**, IL-1β in BMDMs incubated in normoxia or hypoxia for 24 h then LPS for 24 h. **c**, *Il1b* mRNA in LPS-stimulated BMDMs pre-treated with or without α-KG derivative[30] (1 mM). **d**, LPS-induced HIF-1α and IL-1β in BMDMs pre-treated with or without α-KG (0.01, 1, 100, 1000 μM). **e**, LPS-induced IL-1β protein in wild-type (WT) and *Hif1a* deficient (knockout, KO) BMDMs. **f**, ChIP–PCR using HIF-1α antibody and primers specific for −300 position of *Il1b* in LPS-treated BMDMs with or without 2DG (1 mM). **g**, Reporter activity in RAW-264 cells transfected with *Il1b* or −357 *Il1b*. Representative of three experiments. Error bars, s.d. **h**, ChIP–PCR as above in BMDMs treated with LPS with or without α-KG (1 mM). Error bars, s.e.m. $^{**}P < 0.01$.

(Fig. 2d). Induction of IL-1β was attenuated in *Hif1a* deficient macrophages (Fig. 2e).

Inspection of human (*IL1B*) and murine (*Il1b*) gene sequences showed a conserved canonical HIF-1α binding site approximately 300 base pairs upstream from the transcription start site in the human gene, and at position −357 in the mouse gene[4,5]. Chromatin immunoprecipitation (ChIP)–PCR analysis in LPS-stimulated BMDMs showed HIF-1α bound near the −300 position of *Il1b* at 4, 12 and 24 h, which was inhibited by 2DG (Fig. 2f). LPS-induced *Il1b* luciferase activity, which was blocked by 2DG, had substantially reduced activity when −357 in the *Il1b* (Fig. 2g) or −300 in *IL1B* (Supplementary Fig. 9) promoter was mutated. LPS-induced HIF-1α binding to the −300 position of the *Il1b* promoter by ChIP analysis was abolished by pre-treatment with α-KG (Fig. 2h). Therefore IL-1β is a direct target of HIF-1α, with HIF-1α probably having a late effect more associated with the extended expression of IL-1β given the kinetics, supporting previous data[6,7]. The inhibition of IL-1β but not TNF-α induction by 2DG is therefore explained by the HIF-1α dependency in the *IL1B* gene. *Hif1a* deficiency also rescues mice from LPS-induced sepsis[7] but how HIF-1α protein is regulated by LPS is still unknown.

Several groups have shown stabilization of HIF-1α by reactive oxygen species after LPS stimulation[8,9], which we confirmed (Supplementary Fig. 10). Also, HIF-1α is stabilized by the PLC/PKC pathway[9]; however, treatment of BMDMs with specific inhibitors to PLC/PKC had no effect on LPS-induced HIF-1α protein expression at 24 h (Supplementary Fig. 11).

Because both 2DG and α-KG could inhibit HIF-1α accumulation and consequently induction of IL-1β, we considered that the reported change in metabolism induced by LPS must be required for this response. We therefore next examined the metabolic profile of LPS-stimulated BMDMs by flux analysis, a metabolomic screen and microarray analysis. Extracellular flux analysis showed increased glucose use by LPS-stimulated BMDMs (Fig. 3a). This is due to increased glycolysis as measured by an increase in extracellular acidification rate accompanied by a decrease in oxygen consumption rate after LPS stimulation (Fig. 3a and Supplementary Fig. 12), confirming LPS induces the 'Warburg effect' of aerobic glycolysis.

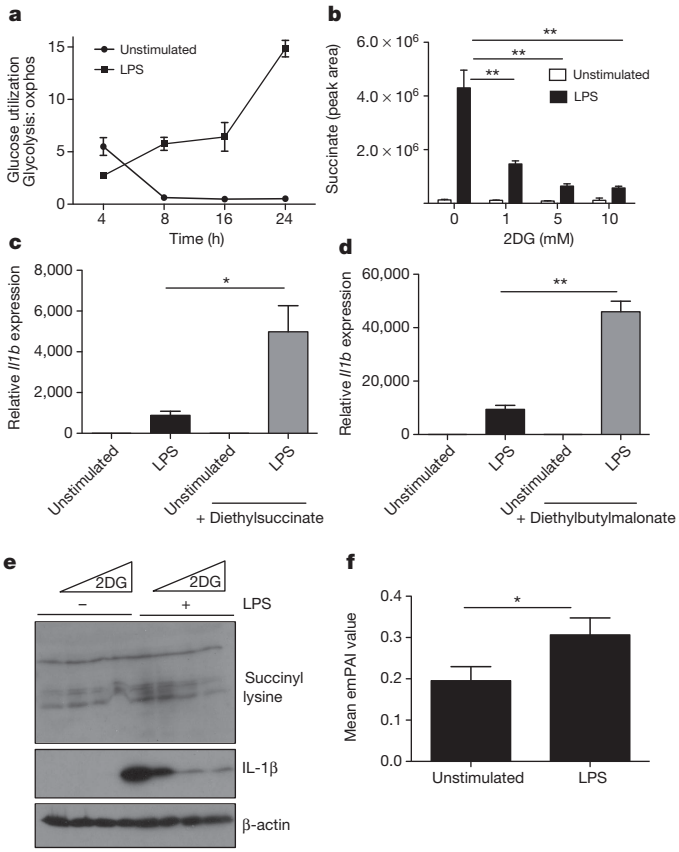

Figure 3 | Succinate is induced by LPS to drive HIF-1α-induced IL-1β expression. **a**, Glucose use over time, as a ratio of extracellular acidification rate/oxygen consumption rate in LPS-treated BMDMs, analysed on the Seahorse XF-24. **b**, Succinate abundance in LPS-stimulated BMDMs pre-treated with or without 2DG (1, 5, 10 mM). **c**, **d**, LPS-stimulated BMDMs pre-treated with or without 5 mM diethylsuccinate or diethylbutylmalonate (1 mM) for 3 h ($n = 3$). **e**, Succinyl-lysine expression and corresponding IL-1β in LPS-stimulated BMDMs with or without 2DG (1, 5, 10 mM) pre-treatment for 3 h. **f**, Mean emPAI values as a measure of relative abundance of proteins listed in Supplementary Table 1. Error bars, s.e.m. $^{*}P < 0.05$; $^{**}P < 0.01$.

The metabolomic screen confirmed this switch in metabolism with 73 metabolites changing out of 208 analysed (Supplementary Fig. 13). Glycolytic intermediates accumulated in 24 h of LPS stimulation. Despite decreased mitochondrial respiration, the tricarboxylic acid (TCA) cycle intermediates fumarate, malate and succinate accumulated. Succinate continued to accumulate between 4 and 24 h, and isocitrate was significantly depleted. Despite a minor increase in citrate at 24 h, there was significant accumulation of di- and triacylglycerols, indicating an increased rate of fatty-acid synthesis. Pentose phosphate pathway intermediates increased, as did the downstream products of purine and pyrimidine metabolism, guanosine, hypoxanthine and inosine (Supplementary Fig. 13). These substrates are necessary to meet the increased demand for energy and nucleic acid synthesis of these highly active cells.

Microarray analysis showed the metabolomic changes correlated with the gene expression profiles of LPS-stimulated BMDMs. Thirty-one metabolic enzyme/transporter-related genes were differentially expressed after 24 h of LPS treatment (Supplementary Fig. 14). The glucose transporters GLUT1, hexokinase 3, 6-phosphofructo-2-kinase/fructose-2,6-biphosphatase 3, phosphoglucomutase-2 and enolase 2 were significantly upregulated, confirming an increase in glycolysis. Lack of mitochondrial activity can be explained by decreased expression of malate dehydrogenase and isocitrate dehydrogenase. In addition, increased amounts of citrate and fatty acids suggested that activity was being diverted away from the TCA cycle for biosynthetic needs. The metabolic screen and flux analysis therefore showed that although there was an overall decrease in TCA cycle activity and mitochondrial respiration at 24 h LPS treatment, there was an accumulation of the key TCA cycle intermediate, succinate.

Further analysis by liquid chromatography–mass spectrometry (LC–MS) showed that LPS caused a 30-fold increase in succinate at 24 h, which equates to an increase in basal succinate from 25 ng to 1 μg per 2×10^6 cells. Pre-treatment with 2DG reduced intracellular succinate, in a dose-dependent manner (Fig. 3b).

Succinate can be transported from the mitochondria through the dicarboxylic acid transporter to the cytosol, where in excess it impairs PHD activity (by product inhibition) leading to HIF-1α stabilization and activation. This phenomenon has been defined as 'pseudohypoxia'[10]. This effect is blocked by α-KG, the substrate for PHD that generates succinate as a by-product in HIF-1α hydroxylation[10,11]. We had observed that α-KG inhibited stabilization of HIF-1α and induction of IL-1β (Fig. 2), indicating that the stabilization of HIF-1α by LPS was probably dependent on the rise of succinate. We tested this further and found that cell-permeable diethylsuccinate alone had no effect on expression of HIF-1α (Supplementary Fig. 15) or *Il1b* (Fig. 3c), because LPS is required to induce *Hif1a* mRNA (Supplementary Fig. 6). However, in combination with LPS, succinate profoundly augmented *Il1b* mRNA expression (Fig. 3c). This supports previous work in which succinate boosted LPS-induced IL-1β in dendritic cells[12]. Succinate amounts are regulated by succinate dehydrogenase. Diethylbutylmalonate, a succinate dehydrogenase inhibitor, increased LPS-induced *Il1b* mRNA (Fig. 3d). Both diethylsuccinate and diethylbutylmalonate increased HIF-1α and IL-1β protein in LPS-treated BMDMs (Supplementary Fig. 15). Diethylsuccinate also increased mRNA of the LPS-induced HIF-1α target *Phd3* (also known as *Egln3*) (ref. 13) (Supplementary Fig. 16). The effect of diethylsuccinate on IL-1β was due to HIF-1α as LPS-stimulated BMDMs from *Hif1a* deficient mice had less IL-1β protein and mRNA than wild type, and pre-treatment with diethylsuccinate had no significant effect. IL-6 and TNF-α were unaffected in *Hif1a* deficient macrophages (Supplementary Fig. 17). Therefore LPS-induced succinate can act as a signal to increase IL-1β expression through HIF-1α.

Certain metabolic enzymes have been shown to undergo succinylation[14]. We observed an increase in succinylation of proteins in response to LPS, which was reduced by 2DG in a dose-dependent manner (Fig. 3e). This was confirmed by a [^{32}P]NAD assay (Supplementary Fig. 18). LPS treatment resulted in a twofold increase in protein succinylation, which was inhibited by 36% with 2DG treatment (data not shown). The expression of *Sirt5* (a recently reported desuccinylase and demalonylase[14]) was inhibited by LPS, suggesting reduced desuccinylase activity (Supplementary Fig. 19). BMDMs treated for 24 h with LPS also had a significantly altered NAD/NADH ratio favouring NADH, thus providing little NAD^+ substrate for SIRT5 activity (Supplementary Fig. 20). This decrease in the NAD/NADH ratio also provides further evidence of enhanced glycolysis and lower respiration. The increase in protein succinylation could therefore be explained by an increase in succinate and a decrease in the expression and activity of the desuccinylase SIRT5.

The relative abundance of proteins in BMDM lysates enriched using a succinyl lysine antibody were detected using LC–MS. Figure 3f represents the mean exponentially modified protein abundance index (emPAI) values (relative quantity) of proteins from unstimulated and LPS-stimulated samples, an enrichment of succinylated proteins being evident in the LPS-treated BMDMs. The increased succinylation of malate dehydrogenase (Supplementary Table 1) has previously been reported in animal tissue[14]. Other proteins identified include glyceraldehyde-3-phosphate dehydrogenase, glutamate carrier 1, L-lactate dehydrogenase A chain and transaldolase. The consequence of succinylation of these proteins, a covalent modification activated by LPS not previously reported, is now under investigation.

A dysfunctional TCA cycle in LPS-stimulated BMDMs pointed towards an alternative source of succinate. The microarray screen showed significantly higher concentrations of glutamine transporter (*Slc3a2*) at 24 h. Succinate can be derived from glutamine through anerplerosis by α-KG. We confirmed LPS induction of *Slc3a2* mRNA (Fig. 4a). *SLC3A2* mRNA expression has previously been shown to increase during intestinal inflammation and is regulated by Sp1 and NF-κB[15]. Blocking the NF-κB pathway with a specific MyD88 inhibitory peptide significantly reduced LPS-induced *Slc3a2* mRNA expression (Supplementary Fig. 21). Knockdown of *SLC3A2* by short interfering RNA in human PBMCs (Supplementary Fig. 22) significantly reduced LPS-induced IL-1β expression (Fig. 4b), but had no effect on IL-6 or TNF-α (Supplementary Fig. 22). This was also demonstrated in the RAW-264 macrophage cell line (Supplementary Fig. 23).

In addition to anerplerosis, succinate can also be derived from glutamine through the 'GABA (γ-aminobutyric acid) shunt' pathway. Gene expression analysis and metabolomics showed LPS-induced GABA transporters (SLC6A13, SLC6A12) and increased GABA production (Supplementary Fig. 13). The increase in GABA was further confirmed by LC–MS (Fig. 4c).

Next we traced the metabolism of [$^{13}C_5$,$^{15}N_2$]glutamine and measured the increase in [$^{13}C_4$]succinate abundance in BMDMs treated with LPS for 24 h (Fig. 4d). This showed a marked increase in succinate production from labelled glutamine. Of the total succinate pool in the LPS-treated BMDMs, 18.4 ± 0.9% ($n = 4$; ± SEM) was labelled after 3 h incubation, as shown by the ratio of [$^{13}C_4$]succinate (heavy labelled succinate) to the sum of all measured succinate isotopomers. This represents a 14-fold increase in succinate relative to non-LPS-treated BMDMs. Treatment of BMDMs with the specific, irreversible inhibitor of the key 'GABA shunt' enzyme GABA transaminase, vigabatrin[16], reduced the percentage of labelled succinate to 16.0 ± 0.6% ($n = 4$; $P = <0.05$), representing a 9.4-fold elevation over the concentrations of succinate attained with vigabatrin alone. This represented a 33% decrease compared with the samples from BMDMs not treated with vigabatrin (Fig. 4e). The elevation in succinate in response to LPS derived from glutamine is therefore largely from anerplerosis by α-KG although a proportion is derived from the 'GABA shunt'.

Pre-treatment of BMDMs with vigabatrin significantly reduced LPS-induced HIF-1α and IL-1β protein (Fig. 4f) as well as *Phd3* mRNA (Supplementary Fig. 24). The inhibitory effect was specific for IL-1β as vigabatrin inhibited *Il1b* mRNA expression (Fig. 4g) but not TNF-α protein amounts or *IL6* mRNA (Supplementary Fig. 24).

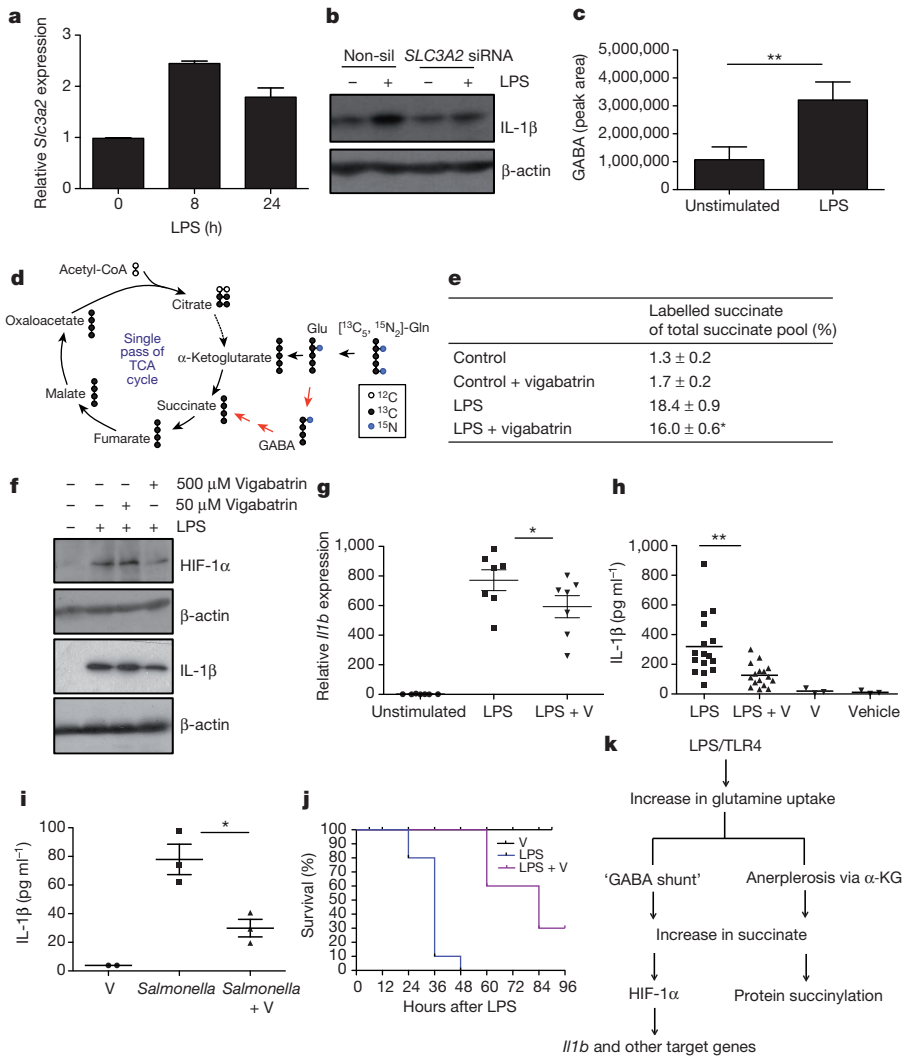

Figure 4 | Glutamine is the source of LPS-induced succinate. **a**, *Scl3a2* mRNA in LPS-treated BMDMs for 8 and 24 h. **b**, IL-1β in human PBMCs transfected with 100 nM *SLC3A2* short interfering RNA compared with non-silencing (non-sil.) control. Representative of three experiments. **c**, GABA abundance in serum-deprived BMDMs stimulated with 10 ng ml^{-1} LPS for 24 h. **d**, Tracing of [$^{13}C_5$,$^{15}N_2$]glutamine in BMDMs treated with LPS for 24 h. **e**, LPS-stimulated BMDMs pre-treated with or without vigabatrin (500 μM) for 20 h then 1 mM [$^{13}C_5$,$^{15}N_2$]glutamine for 4 h. Table represents ratio of [$^{13}C_4$]succinate to the sum of all measured succinate isotopomers as measured by LC–MS. Values are mean ± s.e.m. ($n = 4$). **f**, **g**, LPS-induced HIF-1α and IL-1β protein and *Il1b* mRNA ($n = 7$) in BMDMs pre-treated with or without vigabatrin for 30 min. **h**, IL-1β in serum from mice injected intraperitoneally with or without vigabatrin (400 mg kg^{-1}) or PBS for 1.5 h, then 15 mg kg^{-1} LPS or PBS solution for 1.5 h (LPS, $n = 16$; LPS + vigabatrin (LPS + V), $n = 14$; vigabatrin (V), $n = 3$; vehicle, $n = 3$). **i**, IL-1β in serum from mice injected intraperitoneally with or without vigabatrin (400 mg kg^{-1}) or PBS for 1.5 h then infected with 1×10^6 *Salmonella typhimurium* UK1 intraperitoneally for 2 h. **j**, Survival of mice injected intraperitoneally with or without vigabatrin (400 mg kg^{-1}) or PBS for 1.5 h, then 60 mg kg^{-1} LPS or PBS (PBS, $n = 10$ (not shown); vigabatrin, $n = 10$; LPS, $n = 10$; LPS + vigabatrin, $n = 10$). Error bars, s.e.m. $^*P < 0.05$; $^{**}P < 0.01$. **k**, Proposed model: LPS induces high concentrations of succinate to drive HIF-1α-dependent *Il1b* expression and protein succinylation.

This was also evident *in vivo* as a prescription formulation of vigabatrin (Sabril) reduced LPS-induced IL-1β (Fig. 4h) but had no effect on IL-6 (Supplementary Fig. 25). Similar to 2DG, the inhibitory effect of vigabatrin on TNF-α is probably due to downstream signalling of IL-1β (Supplementary Fig. 25). Similarly vigabatrin reduced IL-1β serum amounts in response to *Salmonella* infection (Fig. 4i). This was consistent with the greater bacterial loading in the spleens of vigabatrin-treated mice (Supplementary Fig. 26). In a model of sepsis, vigabatrin also protected mice, presumably by blocking HIF-1α activation ($P < 0.001$) (Fig. 4j).

Our study therefore shows that chronic activation of macrophages with LPS causes an increase in intracellular succinate by glutamine-dependent anerplerosis and the 'GABA-shunt' pathway. Succinate acts as an endogenous danger signal to stabilize HIF-1α, which in turn specifically regulates gene expression of *Il1b* and other HIF-1α-dependent genes and leads to protein succinylation (Fig. 4k). The role of the 'GABA shunt' is also of substantial interest. Vigabatrin is used clinically to treat epilepsy, as it can increase GABA, which is an inhibitory neurotransmitter. However, adverse effects include significant increased risk of infections[17], which could be caused by limitation of the GABA shunt in macrophages.

Succinate therefore joins other signals derived from mitochondria, including cytochrome C (ref. 18), and mitochondrial DNA[19] that have a role in signalling cell trauma. Succinate can be released to signal through GPR91, which synergizes with Toll-like receptors[12]. High succinate concentrations have been detected in the plasma of patients with peritonitis[20], and in the urine and plasma of diabetic and metabolic disease rodent models[21,22]. In addition, patients harbouring mutations in succinate dehydrogenase have increased HIF-1α activity[23,24] and circulating succinate[25]. Succinate activates HIF-1α in tumours[10,26],

indicating an important similarity between inflammation and cancer. The inflammatory process may have a tumorigenic effect by increasing succinate. The identification of succinate as an inflammatory signal may therefore be important for our understanding of innate immunity in both inflammatory diseases and cancer.

METHODS SUMMARY

Female C57BL/6 mice were from Harlan UK. BMDMs from *Hif1a*$^{flox/flox/LysMcre}$ and wild-type controls, *Hif1a*$^{flox/flox}$ littermate controls, were obtained from M. Whyte. All experiments had previous ethical approval from Trinity College Dublin Animal Research Ethics Committee. BMDMs were prepared as described previously[27]. Unless stated, 100 ng ml^{-1} LPS and 5×10^5 cells per millilitre BMDMs were used in *in vitro* experiments. Two-tailed *t*-tests measured significance of expression of genes with different treatments. Western blot analysis was performed as previously described[28]. Reactive oxygen species were measured on LPS-stimulated BMDMs as previously described[29]. ELISAs for IL-1β (R&D, Quantikine), IL-6 and TNF-α (R&D, Duoset) were performed according to the manufacturer's instructions. Microarray was performed on the Illumina microarray platform. Genes with fold changes in expression greater than 1.5 and Benjamini–Hochberg adjusted *t*-test-based *P* values less than 0.05 were considered significant. Metabolic profiling was in the positive ion MS mode using an LC system. Metabolites with fold change in amounts greater than 10% and *P* values less than 0.05 were considered to be statistically significant. Succinate and GABA amounts were measured by LC–MS analysis. ChIP–PCR using HIF-1α antibody and primers specific for the −300 position of the *Il1b* and *IL1B* genes were performed using a modification of the Millipore/Upstate protocol (MCPROTO407). PBMCs were isolated and transfected with short interfering RNA as described previously[28] using Hs_SLC3A2_1, target sequence AATCCTGAGCCTACT CGAATC (Qiagen). RAW-264 cells were transfected as described previously[28] using Mm_Slc3a2_1 target sequence CAGAAGGATGAAATCAATGAA (Qiagen). The plasmid containing human *IL1B*, pGL3-*IL1* (a gift from J. Kim) and a chloramphenicol acetyltransferase plasmid containing −4093 to +45 of the mouse *Il1b* were mutated using the QuikChange lightning site directed mutagenesis kit (Agilent) according to the manufacturer's instructions. The NAD/NADH ratio was analysed according to the manufacturer's instructions (Biovision K337-100).

Full Methods and any associated references are available in the online version of the paper.

Received 28 March 2012; accepted 5 February 2013.
Published online 24 March 2013.

1. Rodriguez-Prados, J. C. *et al.* Substrate fate in activated macrophages: a comparison between innate, classic, and alternative activation. *J. Immunol.* **185,** 605–614 (2010).
2. Krawczyk, C. M. *et al.* Toll-like receptor-induced changes in glycolytic metabolism regulate dendritic cell activation. *Blood* **115,** 4742–4749 (2010).
3. Pan, H. & Wu, X. Hypoxia attenuates inflammatory mediators production induced by *Acanthamoeba* via Toll-like receptor 4 signaling in human corneal epithelial cells. *Biochem. Biophys. Res. Commun.* **420,** 685–691 (2012).
4. Hiscott, J. *et al.* Characterization of a functional NF-κB site in the human interleukin 1β promoter: evidence for a positive autoregulatory loop. *Mol. Cell. Biol.* **13,** 6231–6240 (1993).
5. Ghisletti, S. *et al.* Parallel SUMOylation-dependent pathways mediate gene- and signal-specific transrepression by LXRs and PPARγ. *Mol. Cell* **25,** 57–70 (2007).
6. Zhang, W. *et al.* Evidence that hypoxia-inducible factor-1 (HIF-1) mediates transcriptional activation of interleukin-1β (IL-1β) in astrocyte cultures. *J. Neuroimmunol.* **174,** 63–73 (2006).
7. Peyssonnaux, C. *et al.* Cutting edge: essential role of hypoxia inducible factor-1α in development of lipopolysaccharide-induced sepsis. *J. Immunol.* **178,** 7516–7519 (2007).
8. Chandel, N. S. *et al.* Reactive oxygen species generated at mitochondrial complex III stabilize hypoxia-inducible factor-1α during hypoxia: a mechanism of O_2 sensing. *J. Biol. Chem.* **275,** 25130–25138 (2000).
9. Sumbayev, V. V. LPS-induced Toll-like receptor 4 signalling triggers cross-talk of apoptosis signal-regulating kinase 1 (ASK1) and HIF-1α protein. *FEBS Lett.* **582,** 319–326 (2008).
10. Selak, M. A. *et al.* Succinate links TCA cycle dysfunction to oncogenesis by inhibiting HIF-α prolyl hydroxylase. *Cancer Cell* **7,** 77–85 (2005).
11. Koivunen, P. *et al.* Inhibition of hypoxia-inducible factor (HIF) hydroxylases by citric acid cycle intermediates: possible links between cell metabolism and stabilization of HIF. *J. Biol. Chem.* **282,** 4524–4532 (2007).
12. Rubic, T. *et al.* Triggering the succinate receptor GPR91 on dendritic cells enhances immunity. *Nature Immunol.* **9,** 1261–1269 (2008).
13. Walmsley, S. R. *et al.* Prolyl hydroxylase 3 (PHD3) is essential for hypoxic regulation of neutrophilic inflammation in humans and mice. *J. Clin. Invest.* **121,** 1053–1063 (2011).
14. Du, J. *et al.* Sirt5 is a NAD-dependent protein lysine demalonylase and desuccinylase. *Science* **334,** 806–809 (2011).
15. Yan, Y., Dalmasso, G., Sitaraman, S. & Merlin, D. Characterization of the human intestinal CD98 promoter and its regulation by interferon-γ. *Am. J. Physiol. Gastrointest. Liver Physiol.* **292,** G535–G545 (2007).
16. Choi, S. & Silverman, R. B. Inactivation and inhibition of γ-aminobutyric acid aminotransferase by conformationally restricted vigabatrin analogues. *J. Med. Chem.* **45,** 4531–4539 (2002).
17. Walker, S. D. & Kalviainen, R. Non-vision adverse events with vigabatrin therapy. *Acta Neurol. Scand.* (suppl.), **124,** 72–82 (2011).
18. Bossy-Wetzel, E., Newmeyer, D. D. & Green, D. R. Mitochondrial cytochrome c release in apoptosis occurs upstream of DEVD-specific caspase activation and independently of mitochondrial transmembrane depolarization. *EMBO J.* **17,** 37–49 (1998).
19. Zhang, Q. *et al.* Circulating mitochondrial DAMPs cause inflammatory responses to injury. *Nature* **464,** 104–107 (2010).
20. Rotstein, O. D., Pruett, T. L. & Simmons, R. L. Lethal microbial synergism in intra-abdominal infections. *Escherichia coli* and *Bacteroides fragilis*. *Arch. Surg.* **120,** 146–151 (1985).
21. Toma, I. *et al.* Succinate receptor GPR91 provides a direct link between high glucose levels and renin release in murine and rabbit kidney. *J. Clin. Invest.* **118,** 2526–2534 (2008).
22. Sadagopan, N. *et al.* Circulating succinate is elevated in rodent models of hypertension and metabolic disease. *Am. J. Hypertens.* **20,** 1209–1215 (2007).
23. Gimenez-Roqueplo, A. P. *et al.* The R22X mutation of the *SDHD* gene in hereditary paraganglioma abolishes the enzymatic activity of complex II in the mitochondrial respiratory chain and activates the hypoxia pathway. *Am. J. Hum. Genet.* **69,** 1186–1197 (2001).
24. Dahia, P. L. *et al.* A HIF1α regulatory loop links hypoxia and mitochondrial signals in pheochromocytomas. *PLoS Genet.* **1,** 72–80 (2005).
25. Hobert, J. A., Mester, J. L., Moline, J. & Eng, C. Elevated plasma succinate in PTEN, SDHB, and SDHD mutation-positive individuals. *Genet. Med.* **14,** 616–619 (2012).
26. Pistollato, F. *et al.* Hypoxia and succinate antagonize 2-deoxyglucose effects on glioblastoma. *Biochem. Pharmacol.* **80,** 1517–1527 (2010).
27. Masters, S. L. *et al.* Activation of the NLRP3 inflammasome by islet amyloid polypeptide provides a mechanism for enhanced IL-1β in type 2 diabetes. *Nature Immunol.* **11,** 897–904 (2010).
28. Doyle, S. L. *et al.* The GOLD domain-containing protein TMED7 inhibits TLR4 signalling from the endosome upon LPS stimulation. *Nature Commun.* **3,** 707 (2012).
29. West, A. P. *et al.* TLR signalling augments macrophage bactericidal activity through mitochondrial ROS. *Nature* **472,** 476–480 (2011).
30. MacKenzie, E. D. *et al.* Cell-permeating α-ketoglutarate derivatives alleviate pseudohypoxia in succinate dehydrogenase-deficient cells. *Mol. Cell. Biol.* **27,** 3282–3289 (2007).

Supplementary Information is available in the online version of the paper.

Acknowledgements We thank the European Research Council, Science Foundation Ireland, the Health Research Board, European Union FP7 programme 'TIMER', Wellcome Trust, National Institutes of Health, Helmsley Trust, Nestle Research Centre, VESKI, The Duquesne University Hunkele Dreaded Disease Award, The Interleukin Foundation and the National Health and Medical Research Council for funding. We also thank R. Thompson for assistance with *Hif1a*$^{-/-}$ mice and M. Murphy for discussions.

Author Contributions G.M.T. designed and did experiments, analysed data and wrote the paper; L.A.J.O. conceived ideas and oversaw the research programme; A.M.C, E.M.P., A.F.M. and J.A. designed and did experiments and analysed data; C.F., N.J.B., B.K., N.H.F., L.Z., A.G., Z.T., S.S.J., S.C.C., S.W., K.P. and F.C.B did experiments; G.G., R.J.X., C.C., M.H. and B.E.C. performed bioinformatic analysis; E.C., V.N., M.W., C.T.T., H.L., S.L.M., E.G., V.K. and C.C., provided advice and reagents; P.E.A. and R.J.X. conceived ideas and oversaw a portion of the work.

Author Information Reprints and permissions information is available at www.nature.com/reprints. The authors declare no competing financial interests. Readers are welcome to comment on the online version of the paper. Correspondence and requests for materials should be addressed to L.A.J.O. (laoneill@tcd.ie).

METHODS

Reagents. LPS used in *in vitro* and *in vivo* studies was from *Escherichia coli*, serotype EH100 (Alexis) and 055:B5 (Sigma-Aldrich), respectively. 2DG (D3179), diethyl succinate (112402), diethyl butylmalonate (112402), vigabatrin (S (+)-γ-vigabatrin, V113), Gö6983 (PKC inhibitor) and *N*-acetyl cysteine (NAC) were all purchased from Sigma, U73122 (PLC inhibitor) from Calbiochem, dimethyloxallyl glycine (71210) from Cayman Chemicals; α-KG was a gift from E. MacKenzie, and Sabril was a gift from L. Cleary. Antibodies used were anti-succinyl lysine (PTM Biolab, PTM-401), anti-IL-1β (R&D, AF401-NA) and anti-HIF-1α (Novus, AF401-NA).

Microarray profiling. Quantification of RNA concentration and purity was measured using a NanoDrop spectrophotometer (Thermo Scientific). The quality of the mouse RNA was ascertained using an Agilent Bioanalyser 2100 with the NanoChip protocol. A total of 500 ng RNA was amplified and labelled using the Illumina TotalPrep RNA Amplification kit (Ambion) according to the manufacturer's instructions. A total of 1.5 μg of labelled cRNA was then prepared for hybridization to the Illumina Mouse WG-6 chip. The Illumina microarray was performed by Partners HealthCare Center for Personalized Genetic Medicine Core.

Cellular respiration and extracellular acidification. An XF24 Extracellular Flux analyser (Seahorse Biosciences) was used to determine the bioenergetic profile of LPS-stimulated BMDMs. BMDMs were plated at 200,000 cells per well in XF24 plates overnight before being stimulated for up to 24 h with LPS. Oxygen consumption rate and extracellular acidification rate were assessed in glucose-containing media (Seahorse Biosciences). Results were normalized to cell number.

Measurement of metabolites by LC–MS. Endogenous metabolic profiling was performed in BMDMs stimulated with LPS for 4 and 24 h with or without 2DG. Polar metabolites were extracted in 80% methanol. Metabolic profiles were obtained using three LC–MS methods. Two separate hydrophilic interaction liquid chromatography (HILIC) methods were used to measure polar metabolites in positive and negative ionization mode MS, and one reversed phase method was used to profile lipids in the positive ion mode. Polar metabolites were profiled in the positive ion MS mode using an LC system comprising a 1200 Series Pump (Agilent Technologies) and an HTS PAL autosampler (Leap Technologies) that was coupled to a 4000 QTRAP mass spectrometer (AB SCIEX) equipped with an electrospray ionization source. Samples were prepared by drying 100 μl of cell extracts under nitrogen and re-suspending the residue in 100 μl of 10/67.4/22.4/0.2 v/v/v/v water/acetonitrile/methanol/formic acid containing stable-isotope-labelled internal standards (valine-d8, Sigma-Aldrich; and phenylalanine-d8, Cambridge Isotope Laboratories). The samples were centrifuged (10 min, 1610*g*, 4 °C), and the supernatants were injected directly onto a 150 mm × 2.1 mm Atlantis HILIC column (Waters). The column was eluted isocratically with 5% mobile phase A (10 mM ammonium formate/0.1% formic acid) for 1 min followed by a linear gradient to 40% mobile phase B (acetonitrile/0.1% formic acid) over 10 min. The ion spray voltage was 4.5 kV and the source temperature was 425 °C. All metabolites were measured using several reaction monitoring scans (MRM). MS settings, including declustering potentials and collision energies, for each metabolite were optimized by infusion of reference standards before sample analyses.

Metabolites labelled with [$^{13}C_5$,$^{15}N_2$]glutamine were analysed using negative ion mode MS performed using an ACQUITY UPLC (Waters) coupled to a 5500 QTRAP triple quadrupole mass spectrometer (AB SCIEX). Cell extracts in 80% methanol were directly injected onto a 150 mm × 2.0 mm Luna NH2 column (Phenomenex) that was eluted at a flow rate of 400 μl min^{-1} with initial conditions of 10% mobile phase A (20 mM ammonium acetate and 20 mM ammonium hydroxide in water) and 90% mobile phase B (10 mM ammonium hydroxide in 75:25 v/v acetonitrile/methanol) followed by a 10 min linear gradient to 100% mobile phase A. The ion spray voltage was −4.5 kV and the source temperature was 500 °C. All data were acquired using MRM scanning. Lipids were profiled in the positive ion mode using an 1100 Series pump and autosampler (Agilent Technologies) coupled to a QSTAR-XL MS system (AB SCIEX).

MultiQuant software (version 1.2; AB SCIEX) was used to process all raw LC–MS data and integrate chromatographic peaks. The processed data were manually reviewed for quality of integration and compared against known standards to confirm metabolite identities.

Succinate and GABA measurements: after stimulations, BMDMs were lysed with a solution kept in dry ice/methanol (−80 °C) composed of 50% methanol and 30% acetonitrile in water and quickly scraped. The insoluble material was immediately pelleted in a cooled centrifuge (0 °C) and the supernatant collected for subsequent LC–MS analysis. A ZIC-HILIC column (4.6 mm × 150 mm, guard column 2.1 mm × 20mm, Merck) was used for LC separation using formic acid, water acetonitrile as component of the mobile phase.

[^{32}P]NAD assay. BMDMs were lysed for 30 min at 4 °C in ice-cold lysis buffer (50 mM Tris-HCl pH 8, 150 mM NaCl, 2 mM EDTA, 0.1% NP-40, 10% glycerol), spun at 1700*g* for 10 min and the supernatant was collected for trypsin digestion. Protein (300 μg) from each sample was dissolved in 6 M guanidine-HCl, 50 mM Tris-HCl (pH 8.0), 15 mM DTT in a reaction volume of 450 μl. Iodoacetamide (1 M, 22.5 μl) was added and the mixture was incubated at room temperature with gentle shaking for 1 h. DTT (1 M, 20μl) was added with gentle mixing for 1 h. Trypsin (10 μg) (Promega, V51111) was added in the final buffer system (50 mM Tris pH 7.4, 1 mM $CaCl_2$) to digest proteins for 16 h at 37 °C. The reaction was quenched by adding 67.5 μl 10% TFA and the digested peptides were desalted by Sep-Pack C18 cartridge (1 cm^3 50 mg^{-1}; Waters) and lyophilized. To detect the protein succinylation concentration in macrophages ± LPS SIRT5 was used to hydrolyse succinyl peptides using [^{32}P]NAD. Reactions were performed in 10 μl solutions with 1 μCi [^{32}P]NAD (ARC, ARP 0141, 800 Ci mmol^{-1}, 0.125 μM), 50 mM Tris-HCl (pH 8.0), 150 mM NaCl, 1 mM DTT. 100 μM synthetic H3K9 succinyl and malonyl peptides were used as positive controls. Macrophage trypsin-digested peptides (100 μg) were used as substrates. The reactions were incubated with 4 μM SIRT5 at 37 °C for 2 h. A total of 0.5 μl of each reaction mixture were spotted onto silica gel thin-layer chromatography plates and developed with 7:3 ethanol: ammonium bicarbonate (1 M aqueous solution). The plates were further air-dried and exposed by PhosphoImaging screen (GE Healthcare) overnight. The signal was detected using a STORM860 phosphorimager (GE Healthcare).

Identification of proteins by LC–MS/MS in a succinyl-lysine pull-down. LPS-treated BMDMs were lysed as above. Anti-succinyl lysine antibody, or non-specific rabbit IgG in the control sample, were pre-coupled to protein A/G agarose beads, washed and incubated with the cell lysates for 2 h at 4 °C. The immune complexes were precipitated and washed thoroughly in lysis buffer. The protein was eluted by adding sample buffer and subsequently separated by SDS–polyacrylamide gel electrophoresis. Gel slices ranging from 35–40 kDa and 55–65 kDa were subjected to one-dimensional nano-scale LC–MS/MS mass spectrometry using an LTQ Orbitrap Velos Pro. Peptides were identified with Mascot (Matrix Sciences) against the Mouse IPI database with a protein score cut-off of 37. The emPAI values of proteins of appropriate molecular mass, excluding non-specifically bound proteins with highest values in the IgG control sample as well as keratin and immunoprecipitation antibody contaminations, were used to estimate relative abundance in the samples. Enrichment of proteins was statistically analysed using an unpaired, two-sided *t*-test for the mean emPAI values.

Endotoxin-induced model of sepsis. Mice were treated ± vigabatrin (400 mg kg^{-1}) or PBS for 30 min. Sepsis was induced by injecting 60 mg kg^{-1} of LPS and survival was monitored. Mice were killed immediately at a humane end-point.